

22.101 Applied Nuclear Physics (Fall 2006)

Lecture 19 (11/22/06)

Gamma Interactions: Compton Scattering

References:

R. D. Evans, *Atomic Nucleus* (McGraw-Hill New York, 1955), Chaps 23 – 25..

W. E. Meyerhof, *Elements of Nuclear Physics* (McGraw-Hill, New York, 1967), pp. 91-108.

W. Heitler, *Quantum Theory of Radiation* (Oxford, 1955), Sec. 26.

We are interested in the interactions of gamma rays, electromagnetic radiations produced by nuclear transitions. These are typically photons with energies in the range of $\sim 0.1 - 10$ Mev. The attenuation of the intensity of a beam of gamma rays in an absorber, sketched in Fig. 17.1, follows a true exponential variation with the distance of penetration, which is unlike that of charged particles,

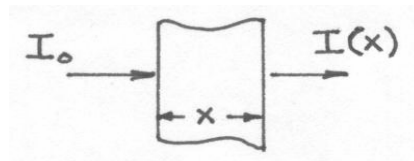


Fig. 17.1. Attenuation of a beam of gamma radiation through an absorber of thickness x .

$$I(x) = I_0 e^{-\mu x} \quad (17.1)$$

The interaction is expressed through the linear attenuation coefficient μ which does not depend on x but does depend on the energy of the incident gamma. By attenuation we mean either scattering or absorption. Since either process will remove the gamma from the beam, the probability of penetrating a distance x is the same as the probability of traveling a distance x without any interaction, $\exp(-\mu x)$. The attenuation coefficient is

therefore the *probability per unit path* of interaction; it is what we would call the macroscopic cross section $\Sigma = N\sigma$ in the case of neutron interaction.

There are several different processes of gamma interaction. Each process can be treated as occurring independently of the others; for this reason μ is the sum of the individual contributions. These contributions, of course, are not equally important at any given energy. Each process has its own energy variation as well as dependence on the atomic number of the absorber. We will focus our discussions on the three most important processes of gamma interaction, Compton scattering, photoelectric effect, and pair production. These can be classified by the object with which the photon interacts and the type of process (absorption or scattering), as shown in the matrix below.

Photoelectric is the absorption of a photon followed by the ejection of an atomic electron. Compton scattering is the inelastic (photon loses energy) relativistic scattering by a free electron. For Compton scattering it is implied that the photon energy is at least comparable to the rest mass energy of the electron. If the photon energy is much lower than the rest mass energy, the scattering by a free electron then becomes elastic (no energy loss), a process that we will call Thomson scattering. When the photon energy is greater than twice the rest mass energy of electron, the photon can be absorbed and an electron-positron pair is emitted. This is the process of pair production. Other combinations of interaction and process in the matrix (marked x) could be discussed, but they are of no interest to us in this class.

<u>Interaction with</u> \	<u>absorption</u>	<u>elastic scattering</u>	<u>inelastic scattering</u>
atomic electron	<i>photoelectric</i>	<i>Thomson</i>	<i>Compton</i>
nucleus	x	x	x
electric field around the nucleus	<i>pair production</i>	x	x

Given what we have just said, the attenuation coefficient becomes

$$\mu = \mu_C + \mu_\tau + \mu_\kappa \tag{17.1}$$

where the subscripts C, τ , and κ will be used henceforth to denote Compton scattering, photoelectric effect, and pair production respectively.

Compton Scattering

The treatment of Compton scattering is similar to our analysis of neutron scattering in several ways. This analogy should be noted by the student as the discussion unfolds here. The phenomenon is the scattering of a photon with incoming momentum $\hbar\mathbf{k}$ by a free, stationary electron, which is treated relativistically. After scattering at angle θ , the photon has momentum $\hbar\mathbf{k}'$, while the electron moves off at an angle φ with momentum \underline{p} and kinetic energy T, as shown in Fig. 17.1.

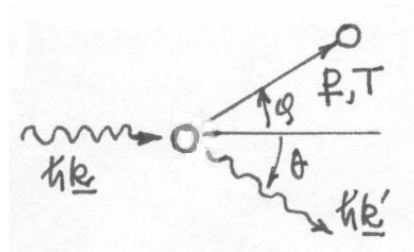


Fig. 17.1. Schematic of Compton scattering at angle θ with momentum and energy transferred to the free electron.

To analyze the kinematics we write the momentum and energy conservation equations,

$$\hbar\mathbf{k} = \hbar\mathbf{k}' + \underline{p} \quad (17.2)$$

$$\hbar ck = \hbar ck' + T \quad (17.3)$$

where the relativistic energy-momentum relation for the electron is

$$cp = \sqrt{T(T + 2m_e c^2)} \quad (17.4)$$

with c being the speed of light. One should also recall the relations, $\omega = ck$ and $\lambda\nu = c$, with ω and ν being the circular and linear frequency, respectively ($\omega = 2\pi\nu$), and λ the wavelength of the photon. By algebraic manipulations one can obtain the following results.

$$\lambda' - \lambda = \frac{c}{\nu'} - \frac{c}{\nu} = \frac{h}{m_e c} (1 - \cos \theta) \quad (17.5)$$

$$\frac{\omega'}{\omega} = \frac{1}{1 + \alpha(1 - \cos \theta)} \quad (17.6)$$

$$T = \hbar\omega - \hbar\omega' = \hbar\omega \frac{\alpha(1 - \cos \theta)}{1 + \alpha(1 - \cos \theta)} \quad (17.7)$$

$$\cot \varphi = (1 + \alpha) \tan \frac{\theta}{2} \quad (17.8)$$

In (17.5) the factor $h/m_e c = 2.426 \times 10^{-10}$ cm is called the Compton wavelength. The gain in wavelength after scattering at an angle of θ is known as the Compton shift. This shift in wavelength is independent of the incoming photon energy, whereas the shift in energy (17.7) is dependent on energy. In (17.6) the parameter $\alpha = \hbar\omega / m_e c^2$ is a measure of the photon energy in units of the electron rest mass energy (0.511 Mev). As $\alpha \rightarrow 1$, $\omega' \rightarrow \omega$ and the process goes from inelastic to elastic. Low-energy photons are scattered with only a moderate energy change, while high-energy photons suffer large energy change. For example, at $\theta = \pi/2$, if $\hbar\omega = 10$ kev, then $\hbar\omega' = 9.8$ kev (2% change), but if $\hbar\omega = 10$ Mev, then $\hbar\omega' = 0.49$ Mev (20-fold change).

Eq.(17.7) gives the energy of the recoiling electron which is of interest because this is often the quantity that is measured in Compton scattering. In the limit of energetic gammas, $\alpha \gg 1$, the scattered gamma energy becomes only a function of the scattering

angle; it is a minimum for backward scattering ($\theta = \pi$), $\hbar\omega' = m_e c^2 / 2$, while for 90° scattering $\hbar\omega' = m_e c^2$. The maximum energy transfer is given by (17.7) with $\theta = \pi$,

$$T_{\max} = \frac{\hbar\omega}{1 + \frac{1}{2\alpha}} \quad (17.9)$$

Klein-Nishina Cross Section

The proper derivation of the angular differential cross section for Compton scattering requires a quantum mechanical calculation using the Dirac's relativistic theory of the electron. This was first published in 1928 by Klein and Nishina [for details, see W. Heitler]. We will simply quote the formula and discuss some of its implications. The cross section is

$$\frac{d\sigma_c}{d\Omega} = \frac{r_e^2}{4} \left(\frac{\omega'}{\omega}\right)^2 \left[\frac{\omega}{\omega'} + \frac{\omega'}{\omega} - 2 + 4 \cos^2 \Theta \right] \quad (17.10)$$

where Θ is the angle between the electric vector $\underline{\varepsilon}$ (polarization) of the incident photon and that of the scattered photon, $\underline{\varepsilon}'$. The diagrams shown in Fig. 17.2 are helpful in visualizing the various vectors involved. Recall that a photon is an electromagnetic wave

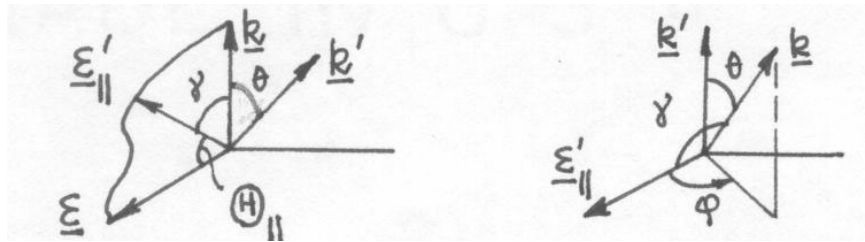


Fig. 17.2. Angular relations among incoming and outgoing wave vectors, \underline{k} and \underline{k}' , of the scattered photon, and the electric vectors, $\underline{\varepsilon}$ and $\underline{\varepsilon}'$, which are transverse to the corresponding wave vectors.

characterized by a wave vector \underline{k} and an electric vector $\underline{\varepsilon}$ which is perpendicular to \underline{k} . For a given incident photon with $(\underline{k}, \underline{\varepsilon})$, shown above, we can decompose the scattered photon electric vector $\underline{\varepsilon}'$ into a component $\underline{\varepsilon}'_{\perp}$ perpendicular to the plane containing \underline{k} and $\underline{\varepsilon}$, and a parallel component $\underline{\varepsilon}'_{\parallel}$ which lies in this plane. For the perpendicular component $\cos \Theta_{\perp} = 0$, and for the parallel component we notice that

$$\cos \gamma = \cos\left(\frac{\pi}{2} - \Theta_{\parallel}\right) = \sin \Theta_{\parallel} = \sin \theta \cos \varphi \quad (17.11)$$

Therefore,

$$\cos^2 \Theta = 1 - \sin^2 \theta \cos^2 \varphi \quad (17.12)$$

The decomposition of the scattered photon electric vector means that the angular differential cross section can be written as

$$\begin{aligned} \frac{d\sigma_c}{d\Omega} &= \left(\frac{d\sigma_c}{d\Omega}\right)_{\perp} + \left(\frac{d\sigma_c}{d\Omega}\right)_{\parallel} \\ &= \frac{r_e^2}{2} \left(\frac{\omega'}{\omega}\right)^2 \left[\frac{\omega}{\omega'} + \frac{\omega'}{\omega} - 2 \sin^2 \theta \cos^2 \varphi \right] \end{aligned} \quad (17.14)$$

This is because the cross section is proportional to the total scattered intensity which in turn is proportional to $(\underline{\varepsilon}')^2$. Since $\underline{\varepsilon}'_{\perp}$ and $\underline{\varepsilon}'_{\parallel}$ are orthogonal, $(\underline{\varepsilon}')^2 = (\underline{\varepsilon}'_{\perp})^2 + (\underline{\varepsilon}'_{\parallel})^2$ and the cross section is the sum of the contributions from each of the components.

In the low-energy (non-relativistic) limit, $\hbar\omega \ll m_e c^2$, we have $\omega' \approx \omega$, then

$$\left(\frac{d\sigma_c}{d\Omega}\right)_{\perp} \sim 0, \quad \left(\frac{d\sigma_c}{d\Omega}\right)_{\parallel} \sim r_e^2 (1 - \sin^2 \theta \cos^2 \varphi) \quad (17.15)$$

This means that if the incident radiation is polarized (photons have a specific polarization vector), then the scattered radiation is also polarized. But if the incident radiation is unpolarized, then we have to average $d\sigma_c / d\Omega$ over all the allowed directions of $\underline{\varepsilon}$ (remember $\underline{\varepsilon}$ is perpendicular to \underline{k}). Since $d\sigma_c / d\Omega$ depends only on angles θ and φ , we can obtain the result for *unpolarized* radiation by averaging over φ . Thus,

$$\begin{aligned} \left(\frac{d\sigma_c}{d\Omega} \right)_{unpol} &= \frac{1}{2\pi} \int_0^{2\pi} d\varphi \left(\frac{d\sigma_c}{d\Omega} \right)_{\text{II}} \\ &= \frac{r_e^2}{2} (1 + \cos^2 \theta) \end{aligned} \quad (17.16)$$

with $r_e \equiv e^2 / m_e c^2 = 2.818 \times 10^{-13}$ cm being the classical radius of the electron (cf. (14.1)). This is a well-known expression for the angular differential cross section for Thomson scattering. Integrating this over all solid angles gives

$$\sigma_c = \int d\Omega \left(\frac{d\sigma_c}{d\Omega} \right)_{unpol} = \frac{8\pi}{3} r_e^2 \equiv \sigma^o \quad (17.17)$$

which is known as the Thomson cross section.

Returning to the general result (17.14) we have in the case of unpolarized radiation,

$$\frac{d\sigma_c}{d\Omega} = \frac{r_e^2}{2} \left(\frac{\omega'}{\omega} \right)^2 \left(\frac{\omega}{\omega'} + \frac{\omega'}{\omega} - \sin^2 \theta \right) \quad (17.18)$$

We can rewrite this result in terms of α and $\cos \theta$ by using (17.6),

$$\frac{d\sigma_c}{d\Omega} = \frac{r_e^2}{2} (1 + \cos^2 \theta) \left(\frac{1}{1 + \alpha(1 - \cos \theta)} \right)^2 \left[1 + \frac{\alpha^2 (1 - \cos \theta)^2}{(1 + \cos^2 \theta) [1 + \alpha(1 - \cos \theta)]} \right] \quad (17.19)$$

The behavior of $d\sigma_c/d\Omega$ is shown in Fig. 17.3. Notice that at any given α the angular distribution is peaked in the forward direction. As α increases, the forward peaking becomes more pronounced. The deviation from Thomson scattering is largest at large scattering angles; even at $\hbar\omega \sim 0.1$ Mev the assumption of Thomson scattering is not

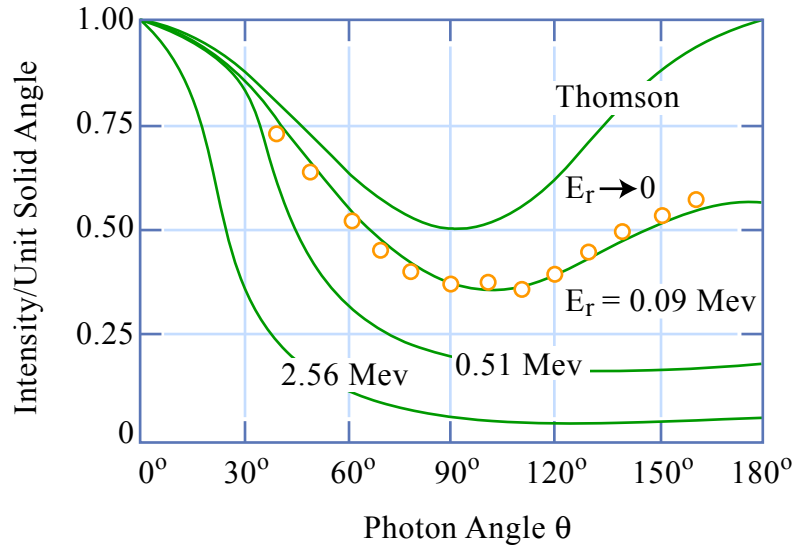


Figure by MIT OCW.

Fig. 17.3. Angular distribution of Compton scattering at various incident energies E_r . All curves are normalized at 0° . Note the low-energy limit of Thomson scattering. (from Heitler)

valid. In practice the Klein-Nishina cross section has been found to be in excellent agreement with experiments at least out to $\hbar\omega = 10m_e c^2$.

To find the total cross section per electron for Compton scattering, one can integrate (17.19) over solid angles. The analytical result is given in Evans, p. 684. We will note only the two limiting cases,

$$\frac{\sigma_c}{\sigma_o} = 1 - 2\alpha + \frac{26}{5}\alpha^2 - \dots \quad \alpha \ll 1$$

$$= \frac{3}{8} \frac{m_e c^2}{\hbar\omega} \left[\ln \frac{2\hbar\omega}{m_e c^2} + \frac{1}{2} \right] \quad \alpha \gg 1$$

(17.20)

We see that at high energies (≥ 1 Mev) the Compton cross section decreases with energy like $1/\hbar\omega$.

Collision, Scattering and Absorption Cross Sections

In discussing the Compton effect a distinction should be made between collision and scattering. Here collision refers to ordinary scattering in the sense of removal of the photon from the beam. This is what we have been discussing above. Since the electron recoils, not all the original energy $\hbar\omega$ is scattered, only a fraction ω'/ω is. Thus one can define a *scattering* cross section,

$$\frac{d\sigma_{sc}}{d\Omega} = \frac{\omega'}{\omega} \frac{d\sigma_C}{d\Omega} \quad (17.21)$$

This leads to a slightly different total cross section,

$$\frac{\sigma_{sc}}{\sigma^o} \sim 1 - 3\alpha + 9.4\alpha^2 - \dots \quad \alpha \ll 1 \quad (17.22)$$

Notice that in the case of Thomson scattering all the energy is scattered and none are absorbed. The difference between σ_C and σ_{sc} is called the Compton *absorption* cross section.

Energy Distribution of Compton Electrons and Photons

We have been discussing the angular distribution of the Compton scattered photons in terms of $\frac{d\sigma_C}{d\Omega}$. To transform the angular distribution to an energy distribution we need first to reduce the angular distribution of two angle variables, θ and φ , to a distribution in θ (in the same way as we had done in Chapter 15). We therefore define

$$\frac{d\sigma_C}{d\theta} = \int_0^{2\pi} d\varphi \frac{d\sigma_C}{d\Omega} \sin\theta = \frac{d\sigma_C}{d\Omega} 2\pi \sin\theta \quad (17.23)$$

and write

$$\frac{d\sigma_c}{d\omega'} = \frac{d\sigma_c}{d\theta} \left| \frac{d\theta}{d\omega'} \right| \quad (17.24)$$

with ω' and θ being related through (17.6). Since we can also relate the scattering angle θ to the angle of electron recoil ϕ through (17.8), we can obtain the distribution of electron energy by performing two transformations, from θ to ϕ first, then from ϕ to T by using the relation

$$T = \hbar\omega \frac{2\alpha \cos^2 \phi}{(1 + \alpha)^2 - \alpha^2 \cos^2 \phi} \quad (12.24)$$

as found by combining (17.7) and (17.8). Thus,

$$\frac{d\sigma_c}{d\Omega_e} 2\pi \sin \phi d\phi = \frac{d\sigma_c}{d\Omega} 2\pi \sin \theta d\theta \quad (12.25)$$

$$\frac{d\sigma_c}{d\phi} = \frac{d\sigma_c}{d\Omega_e} 2\pi \sin \phi \quad (12.26)$$

$$\frac{d\sigma_c}{dT} = \frac{d\sigma_c}{d\phi} \left| \frac{d\phi}{dT} \right| \quad (12.27)$$

These results show that all the distributions are related to one another. In Fig. 17.4 we show several calculated electron recoil energy distributions which can be compared with the experimental data shown in Fig. 17.5.

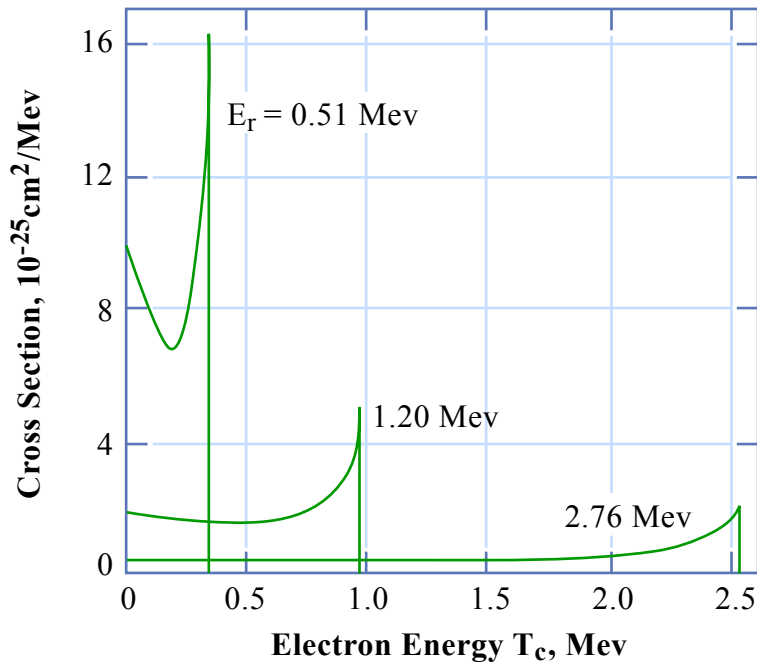


Figure by MIT OCW.

Fig. 17.4. Energy distribution of Compton electrons for several incident gamma-ray energies. (from Meyerhof)

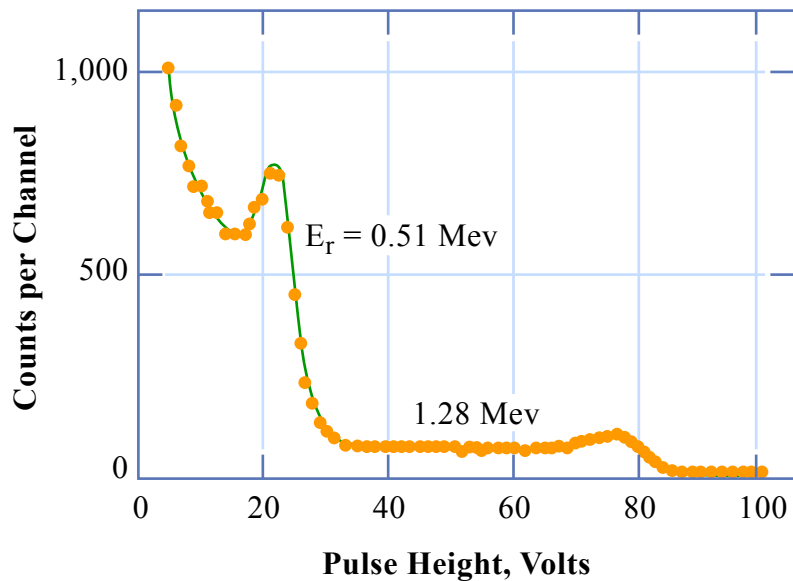


Figure by MIT OCW.

Fig. 17.5. Pulse-height spectra of Compton electrons produced by 0.51- and 1.28-MeV gamma rays. (from Meyerhof)

For a given incident gamma energy the recoil energy is maximum at $\theta = \pi$, where $\hbar\omega'$ is smallest. We had seen previously that if the photon energy is high enough, the outgoing photon energy is a constant at $\sim 0.255 \text{ Mev}$. In Fig. 17.4 we see that for incident photon energy of 2.76 Mev the maximum electron recoil energy is approximately 2.53 Mev , which is close to the value of $(2.76 - 0.255)$. This correspondence should hold even better at higher energies, and not as well at lower energies, such as 1.20 and 0.51 Mev .

We can also see by comparing Figs. 17.4 and 17.5 that the relative magnitudes of the distributions at the two lower incident energies match quite well between calculation and experiment. The distribution peaks near the cutoff T_{\max} because there is an appreciable range of θ near $\theta = \pi$, where $\cos \theta \sim 1$ (cosine changes slowly in this region) and so $\hbar\omega'$ remains close to $m_e c^2/2$. This feature is reminiscent of the Bragg curve depicting the specific ionization of a charged particle (Fig. (14.3)).

From the electron energy distribution $\frac{d\sigma_c}{dT}$ we can deduce directly the photon energy distribution $\frac{d\sigma_c}{d\omega'}$ from

$$\frac{d\sigma_c}{d\omega'} = \frac{d\sigma_c}{dT} \left| \frac{dT}{d\omega'} \right| = \hbar \frac{d\sigma_c}{dT} \quad (12.28)$$

since $\hbar\omega' = \hbar\omega - T$.